MECHANIKA TEORETYCZNA
I STOSOWANA
Journal of Theoretical
and Applied Mechanics
4, 30, 1992

TENSORIAL DAMAGE ANALYSIS OF VISCOELASTIC PLATES

JERZY BIAŁKIEWICZ

ALEKSANDER OLEKSY

Cracow University of Technology

The failure process of a middle–thick plate in linear–viscoelastic constitutive description with the application of tensorial continuum damage mechanics is analysed. The damage evolution is considered on the base of Litewka one parameter model [14]. In the numerical solution of creep of the plate FEM has been used. The numerical investigations are focused on searching the corelation between the incubation time and the damage tensor eigenvalues.

1. Introduction

The safety of engineering structures in creep conditions can be determined by refering the current state to the critical state which is identified with failure. There can be distinguished three periods of time in the damage growth course: time of the first macroscopic cracks in a point, time of the rupture in a cross–section of a structure, and finally, time within which the structure transforms itself into kinetically unsteable mechanism because of either a brittle hinges formation (in rod structures) or brittle break lines (in surface structures). Proposals for safety factors considering both the exploitation and rupture time in the viscoelastic description, either coupled or uncoupled with damage growth, were presented by Chrzanowski et al. [1].

Only in a few exceptional numerical structure analyses in a multiaxial stress state a rupture front propagation causing a deterioration of the load–carrying cross–section had been considered. The examples of such solutions can be found in beams under tension combined with bending [2], in disks [3,4] and plates [5]. That solutions show that relative damage front propagation time referred to the time of rupture does not exceed tens of per cent. Such results partialy justify the limitation of the solutions to the time of the first macroscopic failure in a point (cf [6÷8]). But it should be noticed that the time of failure front propagation in absolute value can be significant and its elimination from considerations is rather a result of mathematical analysis difficulties.

Theoretical rupture model in the above mentioned papers (cf [2÷8]) is based on the damage growth Kachanov–Rabotnov scalar representation ω [9,10] with the critical value $\omega = 1$ in case of failure. A three–dimensional stress state in the damage evlution equation was considered after applying the Sdobyriev–Rabotnov equivalent stress [10]. The constitutive equations are formulated in two ways: in the case of coupled theory with the consideration of net–stresses accounting for the net area damage reduction and for uncoupled theory where nominal stresses are assumed.

The aim of this paper is the rupture analysis of Mindlin plates with the application of the Vakulenko–Kachanov [12] and Murakami–Ohno [13] tensorial damage measure. In this analysis the one parameter damage evolution equation proposed by Litewka [14,15] is assumed. The governing set of equations for the initially–boundary plate problem beside the evolution equation expressed by a density of the elastic strain energy consists of a failure criterion for the solid being damaged [16] and the linear viscoelastic constitutive equation with the omittion of additional strains caused by damage growth.

The numerical analysis will be carried out by the application of FEM in viscoelastic solution and the Runge–Kutta integral procedures in the analysis of damage growth. The solved numerical examples present bending moments and changes of plate deflection during creep as well as redistribution of damage eigenvalue tensor on external planes of the plate with the indication of scratch directions. The numerical solutions indicate that the critical components of damage tensor do not reach unity.

2. Viscoelastic analysis

The plate material is modelled by the linear viscoelastic constitutive equation. In the present paper this material is assumed as the quasi–elastic one. This assumption implies the independence of the first $\nu(t,\tau)$ and the second $\mu(t,\tau)$ Poisson ratios of the load history. Both ratios are then identical functions of the age of the material $(\nu(t) = \mu(t))$ and the constitutive equation can be written in the following form

$$\mathbf{E} = \mathbf{L}\Big[\mathbf{T} - \frac{\nu(t)}{1+\nu(t)}\mathrm{tr}\mathbf{T}\cdot\mathbf{1}\Big] \tag{2.1}$$

where $\mathsf{L}[(\bullet)t]$ is an integral operator

$$\mathsf{L}[(\bullet)t] = \frac{1}{2G(t)}\Big[[(\bullet)t] + \int\limits_{t_0}^{t}[(\bullet)\tau]K(t,\tau)d\tau\Big] \tag{2.2}$$

The material functions $G(t)$ and $K(t,\tau)$, assumed in Eq (2.1), describe the ageing effect and show how the load history affects the current state of strains $(K(t,\tau))$. Further considerations will be based on vector notation of the stress T and strain E tensors. According to the assumptions of the Mindlin–Reissner plate theory [17] vector stress and strain functions will be written down after the bending

$$\boldsymbol{\sigma}_F^{\mathsf{T}} = [\sigma_{xx}, \sigma_{yy}, \sigma_{xy}] \tag{2.3}$$

$$\boldsymbol{\varepsilon}_F^{\mathsf{T}} = [\varepsilon_{xx}, \varepsilon_{yy}, \varepsilon_{xy}] = z\Big[\Theta_{x,x}; \Theta_{y,y}; \frac{1}{2}(\Theta_{x,y} + \Theta_{y,x})\Big] \tag{2.4}$$

and the shear states

$$\boldsymbol{\sigma}_s^{\mathsf{T}} = [\sigma_{xz}, \sigma_{yz}] \tag{2.5}$$

$$\boldsymbol{\varepsilon}_s^{\mathsf{T}} = [\varepsilon_{xz}, \varepsilon_{yz}] = \frac{1}{2}[w_{,x} + \Theta_x; w_{,y} + \Theta_y] \tag{2.6}$$

will have been separated. The variables x, y are rectangular coordinates in the plane of the plate and z is the thickness – direction coordinate measured downwards from the midplane; w is the midplane displacement and Θ_x and Θ_y are the normal rotations in the xz and yz planes, respectively, due to bending. According to the assumptions of the Mindlin plate theory normals to the midplane before deformation remain straight but not necessarily normal to the midplane after deformation.

The creep proces of the plate is analyzed by the application of FEM. The solution will be carried out in established, discrete instants of time t_i by the step Δt

$$t_i = t_0 + i\Delta t \qquad \text{for} \quad i = 0, 1, 2, ..., n \tag{2.7}$$

where t_0 is the instant of loading.

The constitutive equation for each discrete instant of time, after substitution (2.3)÷(2.6) can be written in the form

$$\boldsymbol{\varepsilon}_F(t_i) = \mathbf{M}_F(t_i)\boldsymbol{\sigma}_F(t_i) \tag{2.8}$$

$$\boldsymbol{\varepsilon}_S(t_i) = \mathbf{M}_S(t_i)\boldsymbol{\sigma}_S(t_i) \tag{2.9}$$

In case of statical boundary conditions independent of time, the flexibility matrixes $\mathbf{M}_F(t_i)$ and $\mathbf{M}_S(t_i)$ are multiplied by the integral operator (2.2) computed out from the unity

$$\mathbf{N}_F(t_i) = \frac{1}{2G(t_i)} \begin{bmatrix} \frac{1}{1+\nu(t_i)} & \frac{-\nu(t_i)}{1+\nu(t_i)} & 0 \\ \frac{-\nu(t_i)}{1+\nu(t_i)} & \frac{1}{1+\nu(t_i)} & 0 \\ 0 & 0 & 1 \end{bmatrix} \Big[1 + \int\limits_{t_0}^{t_i} K(t_i,\tau)d\tau\Big] \tag{2.10}$$

$$\mathbf{N}_S(t_i) = \frac{1}{2G(t_i)} \begin{bmatrix} 1 & 0 \\ 0 & 1 \end{bmatrix} \Big[1 + \int\limits_{t_0}^{t_i} K(t_i,\tau)d\tau\Big] \tag{2.11}$$

Applied in this solution the displacement method will require using the inverse (with respect to Eqs (2.8)÷(2.9)) constitutive equations

$$\boldsymbol{\sigma}_F(t_i) = \mathbf{D}_F(t_i)\boldsymbol{\varepsilon}_F(t_i) \tag{2.12}$$

$$\boldsymbol{\sigma}_S(t_i) = \mathbf{D}_S(t_i)\boldsymbol{\varepsilon}_S(t_i) \tag{2.13}$$

In this purpose for each fixed instant of time the flexibility matrixes inversion will be carried out

$$\mathbf{D}_F(t_i) = \mathbf{N}_F(t_i)^{-1} \qquad\qquad \mathbf{D}_S(t_i) = \mathbf{N}_S(t_i)^{-1} \tag{2.14}$$

It should be noticed that the transformation of Eqs (2.8)÷(2.9) into an inverse form (2.12)÷(2.13) in linear–viscoelastic formulation is linked with the necessity to indicate the inverse of the integral operator to (2.2). The analytical form of this operator is defined by the resolvent function $R(t,\tau)$ which is the solution of the integral equation being a relation between the kernel $K(t,\tau)$ and resolvent $R(t,\tau)$. A procedure of the flexibility matrix inversion (2.14) is applied in the present calculations considering the possibility of uniform data preparation (practically in cases when the analytical form of the kernel is related to the numerical form of resolvent).

In the numerical solution of creep the plate is discretized by 9 nodal izoparametric elements of 'heterosis' type, where the shape function is interpolated by the Lagrange's formulas. For the numerical volume integration the Gauss nine point quadrature was applied. The details of the algorithm including the conditions for numerical stability and accuracy can be found in monography [18] (Chapter 6).

The results of creep analysis in course of the damage growth will be presented for the plate material which properties in non-damage state are modeled by the kernel

$$K(t_i,\tau) = \frac{1}{n}\Big(1 - \frac{H}{E}\Big)\exp\Big[-\frac{H}{nE}(t_i - \tau)\Big] \tag{2.15}$$

The analytical form of kernel is related to the creep process limited by asymptote parallel to the time axis. The material constants taken in description characterize: the instantaneous elastic response E, relaxation n and increase of strains caused by creep H. The obtained here results of the numerical solution stresses after transforming to the principle directions are the entrence data for the analysis of the damage process presented in the next paragraph.

3. Damage model

An analysis of a plate damage will be carried out by the application of an one-parameter tensor model in continuum formulation proposed by Litewka [19]. The evolution equation formulating the dependence of the damage rate tensor $\partial_r \boldsymbol{\Omega}$ as a function of a modified stress tensor $\boldsymbol{\sigma}^*$ can be taken in the following form

$$\partial_r \boldsymbol{\Omega} = C\Big[\frac{1-2\nu}{6E}\mathrm{tr}^2\boldsymbol{\sigma} + \frac{1+\nu}{E}\mathrm{tr}\boldsymbol{s}^2 + \frac{D_1}{2(1+D_1)E}\mathrm{tr}\boldsymbol{\sigma}^2\mathsf{D}\Big]^2\boldsymbol{\sigma}^* \tag{3.1}$$

where C is a temperature dependent constant of the material. E and ν are also temperature dependent Young modulus and Poisson ratio for undamaged material whereas $\boldsymbol{s}$ and $\boldsymbol{\sigma}$ are deviator and tensor of stresses, respectively. The magnitude D denotes damage tensor which principle values are defined by the formulas

$$D_i = \frac{S_{ci}}{S_{li}} \qquad \text{for} \qquad i = 1,2,3 \tag{3.2}$$

where S_{ci} and S_{li} stand for the respective crack and ligament areas on the plane orthogonal to the principle directions x_i. The relation between principle values of both damage tensors D and $\boldsymbol{\Omega}$ are related by

$$D_i = \frac{\Omega_i}{1-\Omega_i} \tag{3.3}$$

In modified form of the stress tensor $\boldsymbol{\sigma}^*$ the principle compressing stress components are replaced by zeros, whereas the tensile principle stresses are left unchanged.

A damage in a particle identifies with an instant t_r in which the stress vector (in the 5-dimension space) reaches the surface of a failure criterion for the solid being damaged

$$C_1\mathrm{tr}^2\boldsymbol{\sigma} + C_2\mathrm{tr}\boldsymbol{s}^2 + C_3\mathrm{tr}\boldsymbol{\sigma}^2\mathsf{D} = \sigma_u^2 \tag{3.4}$$

where C_1, C_2 and C_3 are material constants dependent on the temperature and the state of damage growth process. On the other hand σ_u is also the temperature dependent ultimate strength of the undamaged material. The constants C_1, C_2 and C_3 can be determined after the application of Eq (3.4) to three different states of stress: two of uniaxial tension in the perependicular principle directions 1 and

2 and one of equal biaxial tension. These considerations result in three equations with respect to the unknown C_i $(i = 1,2,3)$

$$
\begin{aligned}
C_1 + \frac{2}{3}C_2 + D_1C_3 &= \Big(\frac{\sigma_u}{\sigma_{1u}}\Big)^2 \\
C_1 + \frac{2}{3}C_2 + D_2C_3 &= \Big(\frac{\sigma_u}{\sigma_{2u}}\Big)^2 \\
4C_1 + \frac{2}{3}C_2 + (D_1 + D_2)C_3 &= \Big(\frac{\sigma_u}{\sigma_{bu}}\Big)^2
\end{aligned}
\tag{3.5}
$$

where the ultimate strengths in the uniaxial σ_{1u}, σ_{2u} and biaxial σ_{bu} states can be computed by [20]

$$
\begin{aligned}
\sigma_{1u} &= \sigma_{bu} = (1 - \Omega_1)\sigma_u \\
\sigma_{2u} &= (1 - \Omega_2)\sigma_u
\end{aligned}
\tag{3.6}
$$

The numerical analysis of the plate damage process will be associated with the bending state (2.3) in the present paper. In the considered plane stress state the tensor evolution equation (3.1) is written in a form of a system of equations in the principle stress directions

$$
\begin{aligned}
\partial_\tau \Omega_1 &= \Big[A + B\Omega_1\Big(\frac{\Omega_1}{1-\Omega_1} + m^2 n\frac{\Omega_1}{1-n\Omega_1}\Big)\Big]k\sigma_1^5 \\
\partial_\tau \Omega_2 &= n\partial_\tau \Omega_1
\end{aligned}
\tag{3.7}
$$

where

$$
\begin{aligned}
m &= \frac{\sigma_2}{\sigma_1} \\
A &= 1 - 4\nu m + 2(1 + 2\nu^2)m^2 - 4\nu m^3 + m^4 \\
B &= 2 - 4\nu m + 2m^2 \\
k &= \frac{C}{4E^2}
\end{aligned}
\tag{3.8}
$$

Having in mind the definition of the modified stress tensor σ^* and assuming $\sigma_1 > 0$ in the second damage evolution Eq (3.7) it is needed to consider

$$
n = \begin{cases} m & \text{for} \quad o \leq m \leq 1 \\ o & \text{for} \quad m < 0 \end{cases}
\tag{3.9}
$$

In the plate particles, where both principal stresses are compressive the rates of damage growth (3.7) are equal to zero $(\partial_\tau \Omega_1 = \partial_\tau \Omega_2 = 0)$.

The solution to the set of Eqs (3.7) will be investigated in fixed discrete point pattern on the upper and the bottom plate surfaces, respectively. Data indicating the value of the principal stresses are brought by the viscoelastic plate solution for the assumed uncoupled model of analysis, where in the physical Eq (2.1) the influence of the damage on the deformation increase has been omitted. The Runge–Kutta integral procedures have been applied in the solution to Eqs (3.7) where the material was considered as being undamaged in the initial state

$$\Omega_1(t_0) = \Omega_2(t_0) = 0 \tag{3.10}$$

The integration of Eqs (3.7), for the assumed discretisation of the time axis (2.7), is carried out separately in each of the established points of the plate up till the instant $t_r(x_i)$, in which the damage criterion (3.4) is fulfilled. This criterion, in the considered plane stress state including the conditions defining the constants C_i (3.5) is presented as [14]

$$(1+2m+m^2)C_1 + \frac{2}{3}(1-m+m^2)C_2 + \Big(\frac{\Omega_1}{1-\Omega_1} + \frac{n\Omega_1}{1-n\Omega_1}m^2\Big)C_3 = \Big(\frac{\sigma_u}{\sigma_1}\Big)^2 \tag{3.11}$$

$$\begin{aligned}
&(1-\Omega_1)^2C_1 + \frac{2}{3}(1-\Omega_1)^2C_2 + (1-\Omega_1)\Omega_1C_3 = 1\\
&(1-n\Omega_1)^2C_1 + \frac{2}{3}(1-n\Omega_1)^2C_2 + (1-n\Omega_1)n\Omega_1C_3 = 1\\
&4(1-\Omega_1)^2C_1 + \frac{2}{3}(1-\Omega_1)^2C_2 + 2(1-\Omega_1)\Omega_1C_3 = 1
\end{aligned} \tag{3.12}$$

The time of damage t_r in the point x_i of the plate is adequate for the principal value of damage tensor $\Omega_i < 1$. The state of the damage growth in the analysed points of either the upper or the bottom surfaces of the plate is described by the principal value functions of the damage tensor. For these functions the variables assumed in the middle surface are taken as independent. The numerical analysis of the damage growth – after appearance of the first crack – gives informations related to the directions of crack propagation and the eigenvalue of damage tensor at the damage front.

4. Damage propagation

The results for square plate with uniform distributed load at intensity of $q = 0.15$ kPa will be given here as an example. The kinematic conditions are defined by simple support along the edges AB and BC as well as by restrain with a possibility of a vertical displacement along the edges CD and DA (Fig.1).

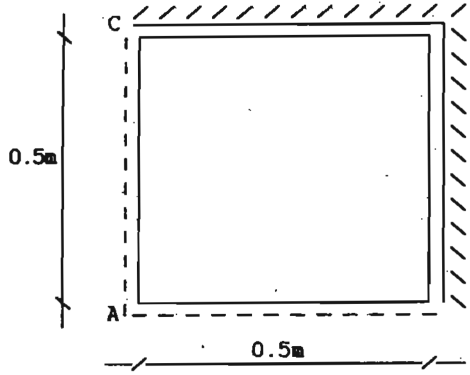

Fig. 1.

In this solution a plate of a constant thickness $h = 0.02$ m and a side length of 0.5 m is considered. The constants that describe the viscoelastic properties of the plate material are physically interpreted in paragraph 2: $E = 0.12$ MPa, $H = 0.06$ MPa and $\nu = 0.47$. Except for that, the damage process course is conditioned by the parameter value $C = 5.97 \cdot 10^{-17}$ and the ultimate strength of the undamaged material $\sigma_u = 288$ MPa. The values of the constants considered here correspond well to the description of the carbon steel behaviour at the temperature of 540^oC.

The analysis of the damage growth process in time is connected with the necessity to integrate the set of ordinary differential Eqs (3.7). In this purpose the Runge–Kutta procedure of the fourth order has been used.

The functions of the midplate deflection are presented in Fig.2. The diagram in Fig.2a shows the immediate elastic deflection at the load instant $t_0 = 0$, while Fig.2b shows the function of the midplate deflection at the instant $t_r = 12000$ h. The deflection increase course in time is noticeable in Fig.3 where the change of the midplane deflection in the point D is presented.

The course of the damage process development is conditioned by the value and the distribution of the cross–sectional forces. The mathematical description of the damage growth is linked with the principal directions of the stress matrix. That is why the diagrams of bending moments have been transformed into principal directions in each of the points of the midplane. The functions of the principal moment distributions (maximal and minimal) are shown in Fig.4a and 4b. The localization of the first macroscopic cracks is linked with the places where the maximal absolute value of bending moments appears.

The process of the damage evolution is illustrated in Fig.5a÷5c. The damage tensor eigenvalue distribution Ω_1 at the instant t_r when the first crack occured (point D: $\Omega_1^{(1)} = 0.57$, $t_r^{(1)} = 205.6 \cdot 10^3 h$) is presented in Fig.5a. The damage concentration in neighbourhood of the point D indicates the development of

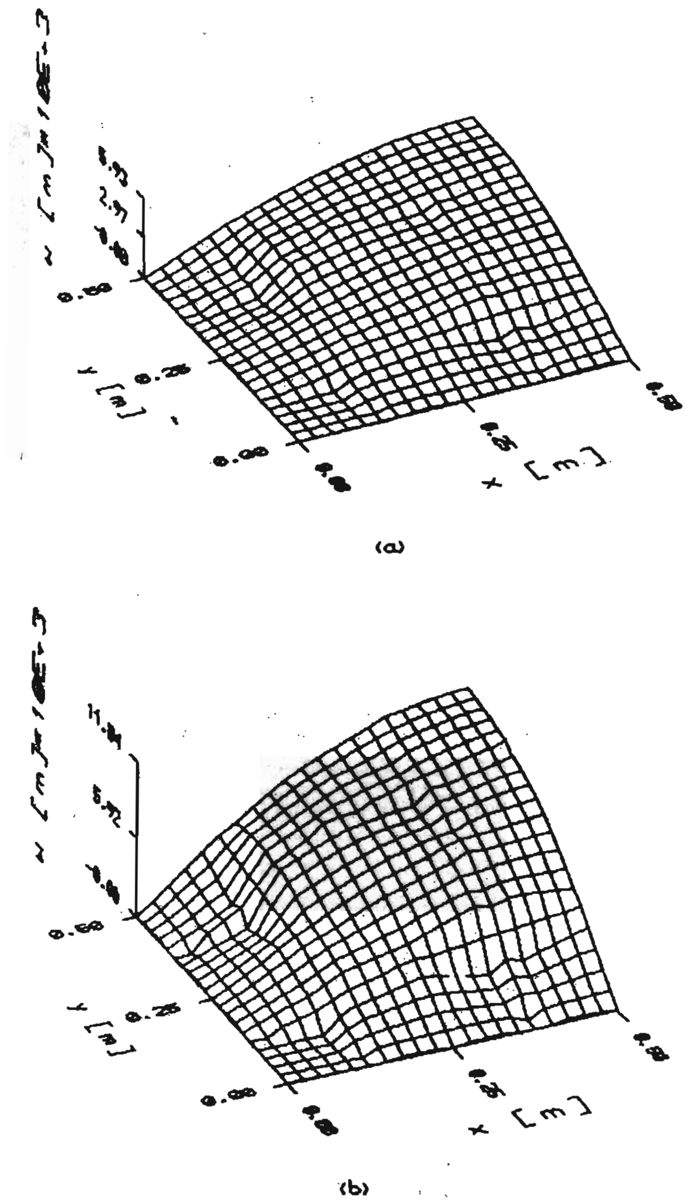

Fig. 2.

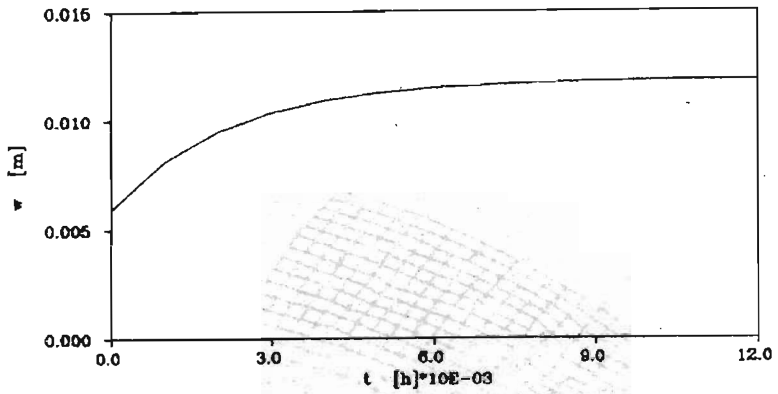

Fig. 3.

the fracture propagation. The chosen stages of the damage process are shown in Fig.5b and 5c where simultaneously consecutive upper indexes of the damage tensor eigenvalues $\Omega_1^{(i)}$ $(i = 1, 2, ...)$ point the actual localization of the rupture front. As it can be seen from the distribution of the damage tensor eigenvalues the development of the failure is associated with the growth of principal values of damage on the rupture front. If the first crack at instant $t_r^{(1)} = 205.6 \cdot 10^3 h$ (point $D \equiv 1$, for taken discretization) corresponds with the eigenvalue $\Omega_1^{(1)} = 0.57$ then at instant $t_r^{(6)} = 720 \cdot 10^3 h$, when the rupture front reaches point 6, the failure proceeds at $\Omega_1^{(6)} = 0.76$.

The influence of the load q on the damage eigenvalue $\Omega_1^{(1)}$ at the instant of the first crack (point D in the external plate surface) is shown in Fig.6. The results of calculations indicate here that the magnitude of the damage principal value will increase when the load q is decreased. The dependence of the eigenvalue $\Omega_1^{(1)}$ on the cross–sectional forces becoming changeable by the side plate dimension (for $q = 0.15$ kPa) is presented in Fig.7. Analogically to the results of calculations presented in Fig.6 it is seen that the decrease of the critical value $\Omega_1^{(1)}$ is connected with the increase of the plate dimensions.

The dependence of the time of the first macroscopic crack on the load q and the plate dimension a are presented in Fig.8 and 9. Both diagrams imply the conclusion that the increase of the cross–sectional forces (caused by the increase of the useful load q as well as the side plate dimension a) leads to the shortening of the time of the first crack. This remark together with earlier presented numerical results of computations (Fig.6 and 7) lead to the conclusion that the critical values of damage tensor are closely connected with the time of rupture process. The elongation of the damage cumulation time up till the instant of the first macroscopic

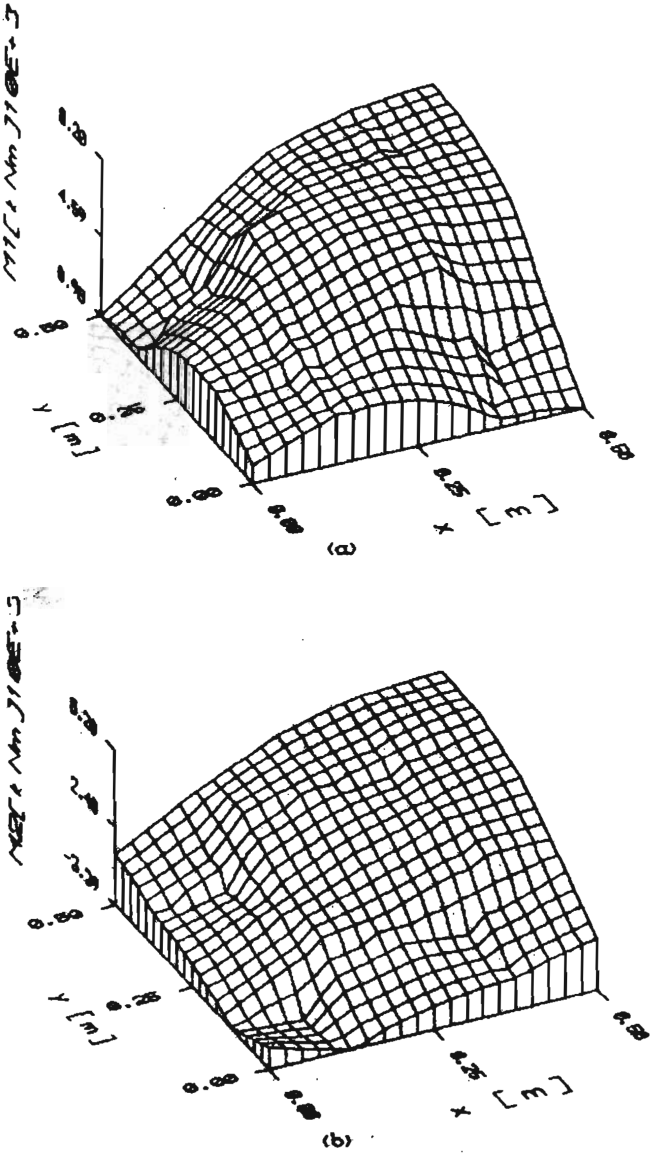

Fig. 4.

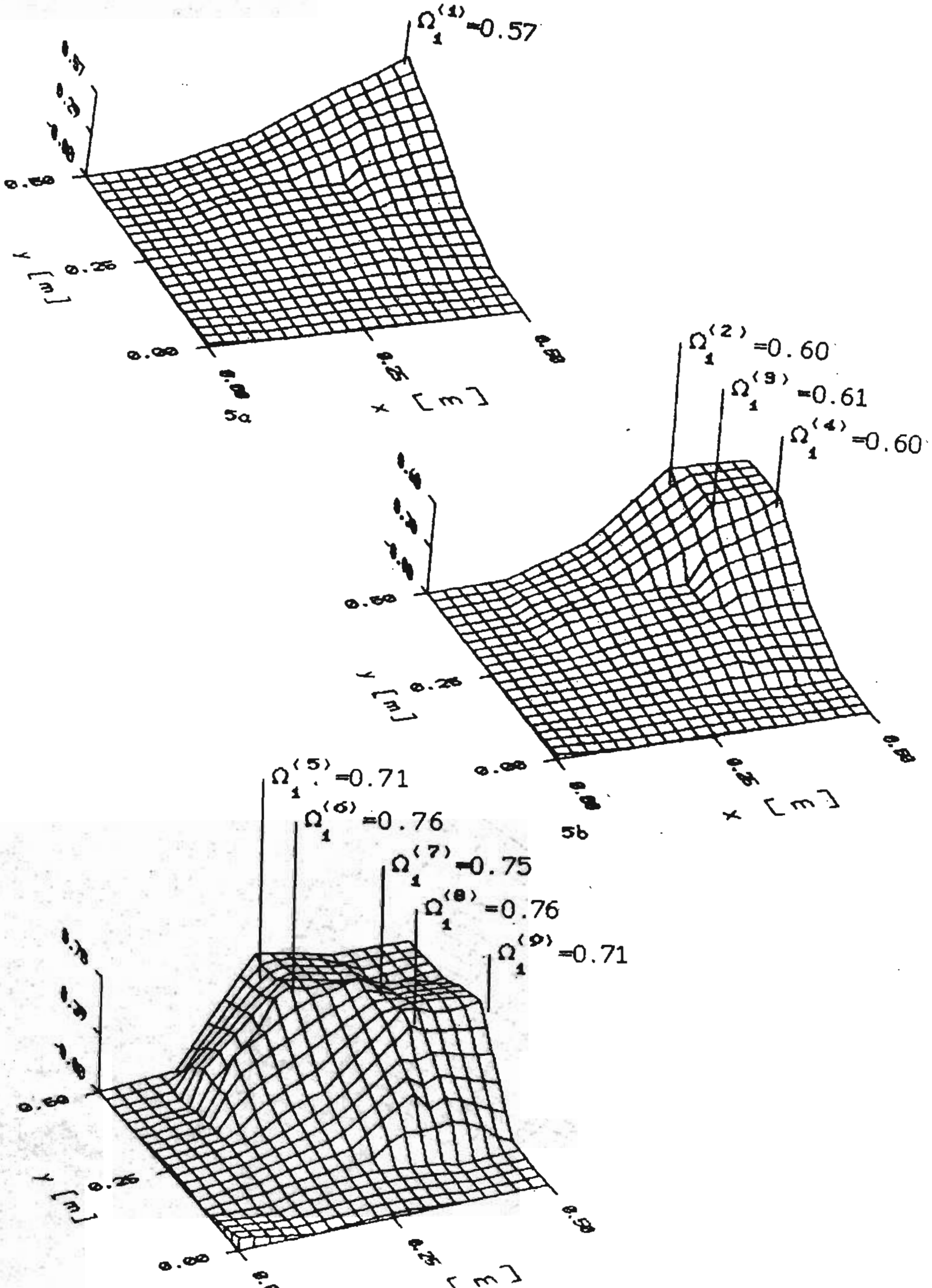

$\Omega_1^{(1)}$=0.57
0.50
y [m]
0.25
0.00
x [m]
5a
$\Omega_1^{(2)}$=0.60
$\Omega_1^{(3)}$=0.61
$\Omega_1^{(4)}$=0.60
0.50
y [m]
0.25
0.00
x [m]
5b
$\Omega_1^{(5)}$=0.71
$\Omega_1^{(6)}$=0.76
$\Omega_1^{(7)}$=0.75
$\Omega_1^{(8)}$=0.76
$\Omega_1^{(9)}$=0.71
0.50
y [m]
0.25
0.00
x [m]
5c

Fig. 5.

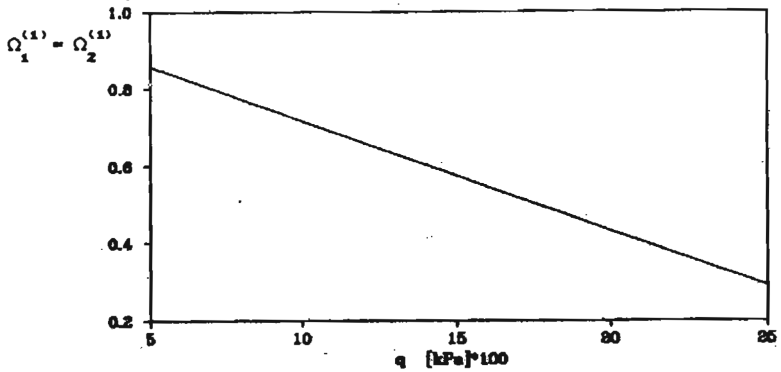

Fig. 6.

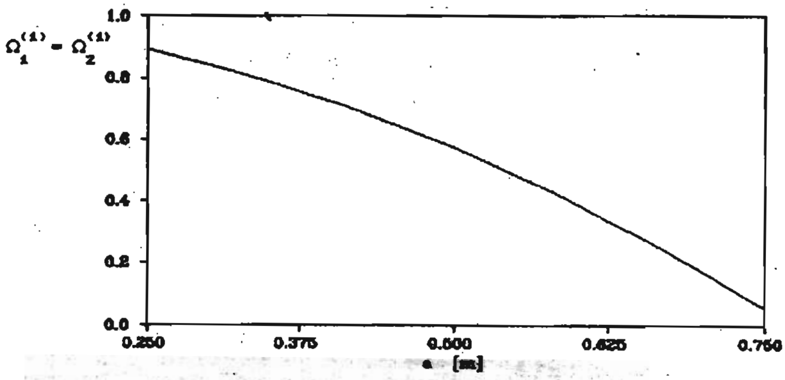

Fig. 7.

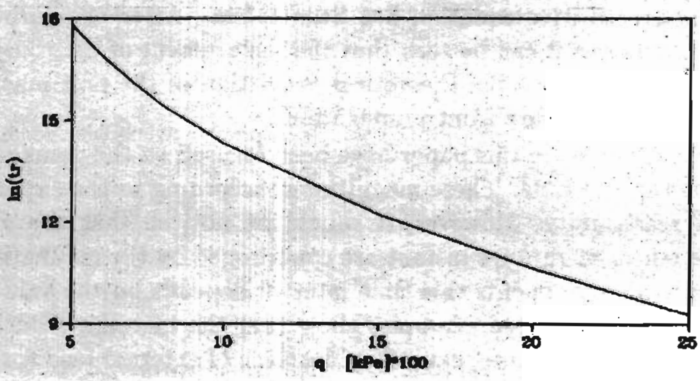

Fig. 8.

crack leads to a higher principal value of damage tensor. In spite of this all the analysed numerical examples prove that these values are considerably less than one ($\Omega_1 = 0.5 \div 0.8$).

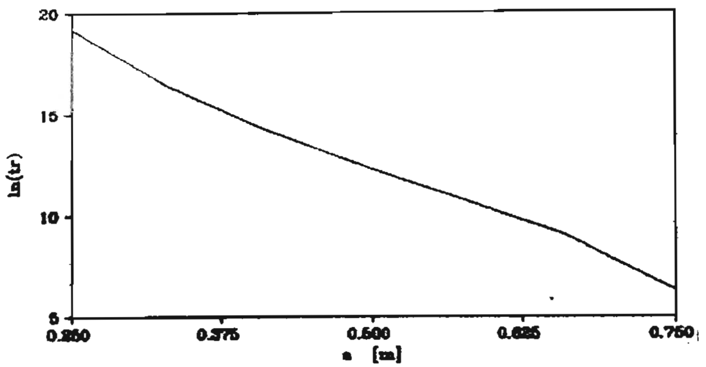

Fig. 9.

5. Final remarks

The experimental data and the results of theoretical investigations set up in Ref. [14] confirm the validity of one parameter model continuum damage mechanics applied in the presented above creep rupture analysis of the plate. Instead of the linear - elastic material model with influences of damage on strain rate the linear viscoelastic constitutive equation has been taken. After comparing both mathematical formulations it can be seen that the replacement of the constitutive description has no influence on the theoretical prediction of the first macrocrack time and afterwards the rupture front propagation.

The main considerations in this paper have been focused on the damage tensor eigenvalues at the rupture time. These magnitudes, according to the expectations (cf [14]), do not reach unity. However, it should be noticed that the principle values of damage tensor at rupture instant are conditioned by the incubation time interval. In structural components this time interval depends on the value of the cross-sectional forces. Computed examples show that the increase of incubation time in fixed point of the structure, caused by decrease of external load (or dimensions of the plate), has the influence on increase of the damage tensor eigenvalues. As it has been pointed out in the preceding paragraph these eigenvalues do not attain unity.

References

1. CHRZANOWSKI M., MADEJ J., LATUS P., 1991, *A CDM motivated safety factor for creeping materials and structures*, 11-th Int.Conf.SMiRT, Tokyo

2. PIECHNIK S., CHRZANOWSKI M., 1970, *Time of total creep rupture of a beam under combined tension and bending*, Int.J.Solids Struct., 6

3. PIECHNIK S., BIAŁKIEWICZ J., 1979, *Ductile-brittle creep, rupture of circulary symmetric disks*, Bull.Ac.Pol., XXVII, 7, 319-325

4. BIAŁKIEWICZ J., 1986, *Dynamic creep rupture of a rotating disk of variable thickness*, Int.J.Mech.Sci., **28**, 10, 671-681

5. BIAŁKIEWICZ J., 1984, *Propagacja frontu zniszczenia kruchego w warunkach pełzania płyt kołowo-symetrycznych*, IX Symp.Reologii Wrocław

6. BODNAR A., 1991, *The influence of failure mechanism mode on the damage field in creeping plates*, 11-th Int.Conf.SMiRT

7. BODNAR A., CHRZANOWSKI M., 1987, *The effect of damage field on the transient creep in plate bending*, Trans.SMiRT-9, L, 273-278

8. BIAŁKIEWICZ., 1984, *Parametrization of bending moments in creep analysis of circularly symmetric simple-supported plates*, Rozpr.Inż., 1, 75-85

9. KACHANOV L., 1958, *On time to rupture in creep conditions*, Izv.AN SSSR, O.T.N., 8, 26-31 (in Russian)

10. RABOTNOV Y.N., 1968, *Creep rupture*, Proc. 12th Int.Congress Appl.Mech., ed. M.Hetenyi, W.G.Vincenti, Stanford, 342-349, Berlin

11. RABOTNOV Y.N., 1966, *Creep of constructional elements*, Nauka, Moscow (in Russian)

12. VAKULENKO A.A., KACHANOV L.N., 1971, *Continuum theory of medium with cracks*, Izv.An SSSR, M.T.T., 4, 159-166 (in Rusian)

13. MURAKAMI S., OHNO N., 1981, *A continuum theory of creep and creep damage*, in: Creep in Structures, ed. A.R.S.Ponter, D.R.Hayhurst, Springer, Berlin, 422-444

14. LITEWKA A., HULT J., 1989, *One parameter CDM model for creep rupture prediction*, Eur.J.Mech.,A/Solids, 8, 3, 185-200

15. LITEWKA A., 1989, *Creep rupture of metals under multi-axial state of stress*, Arch.Mech., 41, 1, 3-23

16. LITEWKA A., 1986, *On stiffnes and strenght reduction of solids due to crack development*, Engng.Fract.Mech., 25, 637-643

17. MINDLIN R.D., 1951, *Influence of rotary inertia and shear on flexural motions of isotropic elastic plates*, J.Appl.Mech., 18, 31-38

18. HINTON E., OWEN D.R.J., 1977, *Finite element programming*, Academic Press, London

19. LITEWKA A., 1987, *Analytical and experimental study of fracture of damaging solids*, In: Yielding Damage and Failure of Anisotropic Solids IUTAM/ICM Symp.

20. ŻUCHOWSKI R., 1986, *Analysis of failure Processes of metals under conditions of thermal fatigue*, (in Polish), Sci.Papers Inst.Material Sci.and Appl.Mech., Technical Univ.of Wrocław, Monographs 18

Tensorowa analiza zniszczenia płyt lepkosprężystych

Streszczenie

Analizowany jest proces zniszczenia płyty średniej grubości w liniowolepkosprężystym opisie konstytutywnym z zastosowaniem tensorowego modelu kontynualnej mechaniki uszkodzeń. Ewolucja zniszczenia rozważana jest w ramach jednoparametrowego modelu Litewki [14]. W rozwiązaniu numerycznym pełzania płyty posłużono się MES. Badania numeryczne skoncentrowano na poszukiwaniu korelacji pomiędzy czasem inkubacji i wartościami własnymi tensora uszkodzeń.

Manuscript received March 23, 1992; accepted for print April 22, 1992